

deformation is entirely due to shear. Thus the two plots coincide for large shear deformation, as they should.

References

¹ Habip, L. M., "A Survey of Modern Developments in the Analysis of Sandwich Structures," *Applied Mechanics Reviews*, Vol. 18, No. 2, 1965, p. 93.

² Pandalai, K. A. and Patel, S. A., "Natural Frequencies of Orthotropic Circular Plates," *AIAA Journal*, Vol. 3, No. 4, April 1965, pp. 780-781.

Effect of Varying Wall Temperature and Total Temperature on Transition Reynolds Number at Mach 6.8

DAL V. MADDALON*

NASA Langley Research Center, Hampton, Va.

Nomenclature

M	= Mach number
P	= pressure, psia
\dot{q}	= heating rate
R	= Reynolds number
T	= temperature, °R
V	= velocity, fps
x	= longitudinal distance from model leading edge, in.
δ	= boundary-layer thickness, in.

Subscripts

aw	= adiabatic wall conditions (turbulent flow)
e	= boundary-layer edge conditions
o	= stagnation conditions
t	= beginning of transition
tun	= tunnel wall temperature
T	= beginning of turbulent flow (peak heating point)
w	= model wall temperature
∞	= freestream conditions

Superscripts

\sim	= root mean square
--------	--------------------

Introduction

AT hypersonic speeds there is much confusion regarding the trend of transition Reynolds number with wall-to-total-temperature ratio.¹⁻⁴ An investigation of this effect was therefore undertaken at $M_\infty \approx 6.8$ over a comparatively large range of wall-to-total-temperature ratio in the Langley $M_\infty \approx 20$ 22-in. helium tunnel. To obtain different levels of T_w/T_o , investigators using conventional wind tunnels generally vary model wall temperature,² whereas investigators using facilities such as shock tunnels and ranges^{3,4} generally vary stagnation temperature. In the present study, both T_w and T_o were varied while holding Mach number, Reynolds number, and T_w/T_o constant. This was done because it was thought that wall cooling might stabilize the boundary layer, whereas changing total temperature might prove destabilizing by altering the facility's disturbance level. Wagner et al.,⁵ have shown that in unheated flow the freestream disturbance level in the 22-in. facility is a result only of sound radiation from the turbulent nozzle wall boundary layer; however, heating the flow could alter the tunnel's noise level and/or introduce additional disturbance modes such as temperature spottiness. The helium wind

tunnel is unique in this ability to operate at $M_\infty \approx 20$ utilizing both heated and unheated flow.

Test Facility, Model, and Techniques

Experiments were conducted in the Langley $M_\infty \approx 20$ hypersonic helium tunnel. This tunnel has a contoured nozzle and a 22-in.-diam test section. For the present investigation, the model was supported from a floor mount. The freestream Mach number in the test core, though constant at any given stagnation pressure, varied with stagnation pressure from a low of 20.1 at 1015 psia to 21.4 at 2515 psia. A calibration and description of the facility is given in Ref. 6. The local inviscid Mach numbers specified in this study were verified experimentally by static pressure and Pitot pressure measurements at the boundary-layer edge. Test conditions are summarized in Table 1, which includes the freestream disturbance levels measured by Wagner⁵ with a hot wire anemometer in unheated flow (attempts in that study to repeat the hot wire measurements in heated flow were unsuccessful because of repeated wire failures).

The transition model was a sharp leading edge (0.002 in. thick), smooth, flat plate 21 in. long and 14 in. wide. The plate was set at 10° angle of attack; the local Mach number was therefore about 6.8. The model was fabricated of AISI 405 stainless steel with a wall thickness of about 0.030 in. and had swept end plates. This was the same model used in Cary's study² and a more complete model description can be found in this reference. Thirty-four thermocouples placed along the model centerline and spaced about 0.5 in. apart were used to determine heating rates and, thence, transition location. The rate of surface temperature rise was obtained from a second-degree curve fit (by the method of least squares) to the temperature time data for a 0.5-sec time interval starting about 2 sec after flow was established. The length of the run was about 6 sec. Conduction errors were checked and found to be negligible. The beginning of transition $(R_{e,x})_t$ was defined as the point where the \dot{q} vs $R_{e,x}$ curve departed from a laminar $\frac{1}{2}$ power slope, whereas the beginning of turbulent flow (end of transition) $(R_{e,x})_T$ was taken as the peak heating point.

To avoid the problem of frost formation on the model's surface, a 0.002-in.-thick Mylar sheet was placed over the entire surface of the model such that no air gaps existed between the surface and the Mylar sheet. The tunnel was then evacuated to a pressure of about 0.2 mm Hg, and the model internally cooled with liquid nitrogen to the desired wall temperature (generally uniform within $\pm 10^\circ\text{R}$). The gaseous nitrogen was re-routed out of the tunnel and exhausted to the atmosphere. A frost coating estimated at about 0.002-in. thickness formed on top of the Mylar cover when the wall was cooled below 360°R. Immediately before flow was established, the cover was rapidly removed and the run started. This procedure enabled runs to be made with the model completely frost free.

Results

The effect of wall cooling on transition Reynolds number is presented in Fig. 1 for two unit Reynolds numbers where, for a given unit Reynolds number and total temperature, the freestream disturbance level is constant (model wall temperature was independently varied). For unheated flow the measured disturbance levels of Ref. 5 are included in Table 1. Considering first the data obtained in unheated flow (open symbols), both $(R_{e,x})_t$ and $(R_{e,x})_T$ are seen to decrease continuously from $T_w/T_o \approx 0.3$ to $T_w/T_o \approx 0.8$ with no transition reversal evident within this wall-to-total-temperature ratio range. This is the same trend observed by Cary.² A further increase past the adiabatic wall temperature ratio to $T_w/T_o \approx 0.95$, however, results in a pronounced increase in the transition location. In this case the plate is transferring heat to the flow. The sharp increase

Received August 15, 1969.

* Aerospace Engineer, Flow Analysis Section.

Table 1 Summary of test conditions

Flow	P_o	M_∞	M_e	$R_e/\text{in.} \times 10^{-6}$	R_e/R_∞	V_e	T_o	T_{tun}/T_o	$(\bar{P}/P)_\infty^2$	$(\bar{m}/m)_\infty$	$(\bar{T}_o/T_o)_\infty$
Unheated	1015	20.1	6.8	0.324	0.88	5740	563	0.96	0.00238	0.0290	0.0004
Unheated	1515	20.5	6.8	0.460	0.87	5750	566	0.95	0.00161	0.0234	0.0013
Heated	1515	20.5	6.8	0.317	0.87	6860	804	0.67	—	—	—
Heated	2515	21.4	6.9	0.459	0.83	6860	803	0.67	—	—	—

in transition Reynolds number occurs for both unit Reynolds numbers and is evident not only in the beginning of transition $(R_{e,x})_i$, but also in the end of transition $(R_{e,x})_T$. This is a new type of transition reversal which is unexplained by existing theories, and it occurs without any change in the tunnel wall boundary layer. One possible explanation for this behavior is that for $T_w/T_o < 0.88$ the model nose is relatively hot, whereas for $T_w/T_o > 0.88$ the model nose is relatively cool. Especially designed check runs were therefore made with a model temperature difference ahead of $(R_{e,x})_i$, as large as 50°R (both positive and negative 50°R) and these tests indicated a negligible effect of this limited temperature difference on $(R_{e,x})_i$ and $(R_{e,x})_T$. Lower speed results⁷⁻⁹ had indicated that for increases in wall-to-total-temperature ratio above adiabatic conditions, $(R_{e,x})_i$ would decrease with increasing T_w/T_o .

Data from a previous investigation⁵ in this facility on an equivalent model (a 10° wedge) are included in Fig. 1 and show close agreement with the present data. Estimates of δ based on laminar theory also were computed for various T_w/T_o ratios and indicated that $(R_{e,\delta})_i$ increased as T_w/T_o increased from 0.3–0.8. This result suggests that the trend of transition Reynolds number with t_w/t_o depends on the reference length used.

The heated flow data (closed symbols) show the same trend as the unheated data in that $(R_{e,x})_i$ and $(R_{e,x})_T$ both decrease with increasing wall-to-total-temperature ratio from $T_w/T_o \approx 0.23$ to 0.67 with no evidence of a transition reversal in this temperature ratio range. The length of the transition region also was examined in heated and unheated flow, and it was found that the transition length was approximately equal to the length of the laminar flow region [i.e., $(R_{e,x})_T \approx 2(R_{e,x})_i$].

Turning now to a comparison of the data obtained in heated and unheated flow, it is evident at both $R_e/\text{in.} \approx 0.32 \times 10^6$ and $R_e/\text{in.} \approx 0.46 \times 10^6$ that $(R_{e,x})_i$ and $(R_{e,x})_T$ are independent of the tunnel stagnation temperature. The transition Reynolds numbers obtained in unheated flow agree with the transition Reynolds numbers obtained in heated

flow at all T_w/T_o ratios studied. These results suggest that, for the present data obtained in heated flow, sound rather than temperature spottiness is the dominant disturbance mode. Had temperature spottiness been dominant it would be expected to raise the freestream disturbance level which would result in $(R_{e,x})_i$ being lower in heated flow than in unheated flow. It is mentioned, however, that among the unknown effects of heated flow are the different boundary-layer edge velocities, the influence of the model shock wave, and a possible changed noise level occurring because of a different tunnel wall boundary layer. It is also recognized that temperature spottiness may not be negligible in a truly high-temperature facility.

Mack¹⁰ has suggested that for air (which obeys the Sutherland viscosity relation over a large temperature range) total temperature itself may be a parameter affecting transition location. This argument is not relevant to the present data since the viscosity of helium obeys a power law variation with temperature for the present range of test conditions.

Conclusions

- 1) With M_e , $R_e/\text{in.}$, and T_w/T_o held constant, transition Reynolds numbers were measured in both moderately heated and unheated flow. $(R_{e,x})_i$ and $(R_{e,x})_T$ were found to be independent of the stagnation temperature. This result indicated that sound, rather than temperature spottiness, was the dominant mode in heated as well as unheated flow.
- 2) With M_e , $R_e/\text{in.}$, and T_o held constant (and therefore a fixed freestream disturbance level), $(R_{e,x})_i$ and $(R_{e,x})_T$ significantly decreased with increasing temperature ratio in the range $T_w/T_o = 0.2$ to 0.8. In unheated flow, where data were available above adiabatic wall temperature, a new type of transition reversal occurred.
- 3) In both heated and unheated flow, there was no transition reversal at the lowest wall-to-total-temperature ratios reached in this study.

References

- 1 Morkovin, M. V., "Critical Evaluation of Transition From Laminar to Turbulent Shear Layers With Emphasis on Hypersonically Traveling Bodies," TR-68-149, March 1969, Air Force Flight Dynamics Lab.
- 2 Cary, A. M., Jr., "Turbulent Boundary-Layer Heat Transfer and Transition Measurements for Cold-Wall Conditions at Mach 6," *AIAA Journal*, Vol. 6, No. 5, May 1968, pp. 958–959.
- 3 Stetson, K. F. and Rushton, G. H., "Shock Tunnel Investigation of Boundary-Layer Transition at $M = 5.5$," *AIAA Journal*, Vol. 5, No. 5, May 1967, pp. 899–906.
- 4 Sheetz, N. W., "Free-Flight Boundary-Layer Transition Investigations at Hypersonic Speeds," AIAA Paper 65-127, New York, 1965.
- 5 Wagner, R. D., Jr. et al., "Influence of Measured Free-Stream Disturbances on Hypersonic Boundary-Layer Transition," AIAA Paper 69-704, San Francisco, 1969.
- 6 Arrington, J. P., Joiner, R. C., Jr., and Henderson, A. Jr., "Longitudinal Characteristics of Several Configurations at Hypersonic Mach Numbers in Conical and Contoured Nozzles," TN D-2498, 1964, NASA.
- 7 Scherrer, R., Wimbrow, W. R., and Gowen, F. E., "Heat Transfer and Boundary-Layer Transition on a Heated 20° Cone at a Mach Number of 1.53," RM A8L28, 1949, NACA.
- 8 Scherrer, R., "Boundary-Layer Transition on a Cooled 20° Cone at Mach Numbers of 1.5 and 2.0," TN 2131, 1950, NACA.

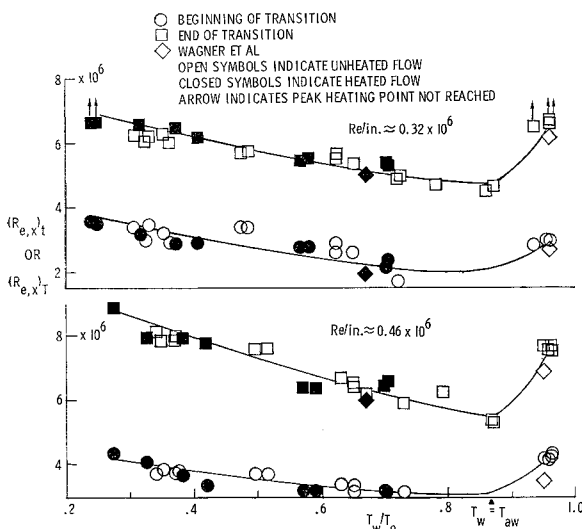


Fig. 1 Effect of T_w/T_o on transition in heated and unheated flow at $M_e \approx 6.8$.

⁹ Higgins, R. W. and Pappas, C. C., "An Experimental Investigation of the Effect of Surface Heating on Boundary-Layer Transition on a Flat Plate in Supersonic Flow," TN 2351, April 1951, NACA.

¹⁰ Mack, L. M., "Effect of Free-Stream Temperature on the Inviscid Stability of the Compressible Laminar Boundary Layer," Space Programs Summary 37-39, Vol. IV, June 1966, Jet Propulsion Lab., pp. 145-146.

Evaluation of Electron Quench Additives in a Subsonic Air Arc Channel

K. E. STARNER*

The Aerospace Corporation, El Segundo, Calif.

I. Introduction

DECREASING the electron concentration of high-temperature flowing plasmas is useful toward improving communications with, and reducing, the radar observables produced by re-entry vehicles. The addition of small quantities of an electrophilic gas such as SF_6 to the ionized flow is a known effective method of electron removal from gases below 1000°K .¹ Electrophilic gases suppress the electron concentration of plasmas by electron attachment, with subsequent negative ion formation. Major questions concerning high-temperature effects, reaction rates, and flow transit times must be answered if such an electron-removal technique is to be used successfully on re-entry vehicles. Thus, screening tests in high-temperature flows are helpful in comparing the electron removal effectiveness of candidate quench additives.

High-temperature ionized flows can be produced in the laboratory using electrical arc jet facilities. The results of quenchant tests performed in a supersonic argon arc jet are given in Ref. 2. In the present study, a subsonic arc channel was used to provide a flowing high-temperature air plasma in which the electrophilic effects of various additives could be studied under simulated flight conditions. It was possible to monitor the electron concentration of the flow before and after quench injection, thus allowing direct comparison of the electron removal capability of many additives. This Note describes the experiments conducted, and presents results obtained using a variety of candidate additives.

II. Facility Description

A schematic of the d.c. arc channel arranged for quench experiments is shown in Fig. 1 and is described in detail in Ref. 3. The arc discharge is struck in the nitrogen flow through the anode region and is mixed with oxygen immediately downstream to produce an air plasma. The 2×0.5 -in. rectangular arc channel begins downstream of a constant area circular-to-rectangular transition section. Enclosure of the plasma in a water-cooled heat balance channel permits evaluation of many flow, thermodynamic, and electrical properties at the axial location of interest. Also, in such a channel the large effective length-to-diameter ratio permits flow mixing in a controlled velocity environment.

Received June 5, 1969; revision received July 18, 1969. This work was supported by the U.S. Air Force under Contract F04701-68-C-0200. The author gratefully acknowledges the contribution of W. P. Thompson, who supervised the use of microwave diagnostic equipment and T. L. Felker and H. A. Bixler, who operated the arc facility.

* Member of the Technical Staff, Aerodynamics and Heat Transfer Department, Aerodynamics and Propulsion Laboratory.

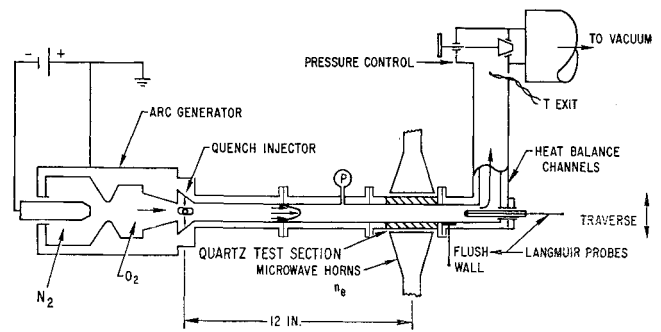


Fig. 1 Arc channel schematic.

For the tests of this study, the basic arc channel arrangement consisted of a quench injector station followed by two 4-in.-long channel sections plus a 4-in.-long interchangeable test section with selectable chambers comprised of either quartz or copper sidewalls. The channel was terminated by a heat exchanger and flow control valve at the vacuum duct. Quenchant was injected in several ways using midstream crossflow, centerline axial flow, and flush wall injection techniques in different arc runs. Additional details of the channel are given in Ref. 4.

III. Flow Diagnostics

The average enthalpy of the plasma at several axial channel locations can be determined by using the heat balance segments. Stream bulk average enthalpy is decreased by about a factor of 2 due to cold wall heat transfer as it traverses the 12-in. distance downstream of the additive injector. Typical equilibrium profiles of velocity, enthalpy, ion number density, and temperature calculated from probe measurements made across the 0.5-in. channel dimension are given in Ref. 3. A calculated ratio of centerline to average enthalpy of 1.37 was found, and is in good agreement with the analysis of Ref. 5.

Integrated electron number density across the 0.5-in. channel dimension was determined by using X- or S-band microwave interferometer systems⁶ in conjunction with the quartz test section walls. Use of such a system is confined to a limited electron number density range which, in these tests, limited the maximum monitoring range to about a factor of 10. At electron concentrations below the lower sensitivity limit of the microwave equipment, Langmuir probe measurements were used. Both flush wall and free-stream stagnation point continuum Langmuir probes were mounted immediately downstream of the microwave test section as illustrated in Fig. 1. The single electrode Langmuir probes were referenced to the channel and measured from positive through negative saturation currents as the applied voltage E was swept through negative-to-positive 50 v. Probe positive saturation current was repeatedly confirmed to be directly proportional to electron number density in the unquenched plasma by comparison of probe and microwave data.

Figure 2 shows the type of Langmuir probe trace obtained prior to and subsequent to each significant decrease in n_e due to quenching as observed over the dynamic range of the microwave interferometer. The major effect observed at the probes was a large decrease (up to several orders of magnitude) in negative saturation current to a value nearly equal to that for positive saturation, resulting in a symmetrical probe characteristic. If we assume positive saturation current proportional to the product of ion mean speed and positive charge number density at the sheath edge,[†] and negative saturation current proportional to the sum of similar

[†] This proportionality has been found to hold⁷ for a continuum probe when the ion sheath thickness is somewhat larger than the ionized-neutral gas mean free path as calculated for these tests.